

Signatures for Majorana neutrinos in $e^- \gamma$ collider

J.Peressutti and O.A.Sampayo

*Departamento de Física, Universidad Nacional de Mar del Plata
Funes 3350, (7600) Mar del Plata, Argentina*

Jorge Isidro Aranda

*Escuela de Ciencias Físico-Matemáticas,
Universidad Michoacana de San Nicolas de Hidalgo,
Morelia, Michoacan, Mexico.*

Abstract

We study the possibilities to detect Majorana neutrinos in $e^- \gamma$ colliders for different center of mass energies. We study the $W^- W^- l_j^+ (l_j^+ \equiv e^+, \mu^+, \tau^+)$ final state which are, due to leptonic number violation, a clear signature for intermediate Majorana neutrino contribution. Such a signal (final lepton have the opposite charge of the initial lepton) is not possible if the heavy neutrinos are Dirac particles. In our calculation we use the helicity formalism to obtain analytic expressions for the amplitude and we have considered that the intermediate neutrinos can be either on shell or off shell. Finally we present our results for the total cross-section and for the angular distribution of the final lepton. We also include a discussion on the expected events number as a function of the input parameters.

I. INTRODUCTION

Massive neutrinos can come in two different types: as Dirac or Majorana particles. Dirac fermions have distinct particles and antiparticle degrees of freedom while Majorana fermions make no such distinction and have half as many degrees of freedom. In this conditions fermions with conserved charges (color, electric charged, lepton number,...) must be of Dirac type, while fermions without conserved charges may be of either type. If the neutrino mass vanishes then both types are equivalent to two-component Weyl fermions and the distinction between Dirac and Majorana neutrinos vanishes [1]. New neutrinos could have large masses and be of either type. If there are heavy neutrinos, then the present and future experiments offer the possibility of establishing their nature. The production of Majorana neutrinos via e^+e^- and hadronic collision have been extensively investigated in the past [2–7]. In this work we study the possibility of the γe^- linear collider to produce clear signatures for Majorana neutrinos. The photon linear collider [8] may be the best alternative to the electron positron colliders and furthermore, in the case of Photon linear collider, we can control the initial photon polarization by the inverse Compton scattering of the polarized laser by the electron beam at NLC. Using these polarized high energy photon beam we have the possibility to study in detail the interaction of Majorana neutrinos and reject possible background. In this paper we discuss the signatures for Majorana neutrinos in the reactions $\gamma e^- \rightarrow W^-W^-l_j^+(l_j^+ \equiv e^+, \mu^+, \tau^+)$. For the cross section calculation we have used the helicity formalism. The phase space integration was done taking account that the intermediate neutrinos can be either on shell or off shell. Due the large CM energies of these colliders we have considered that the mass of the final lepton vanishes. Moreover we study distributions of the final leptons for different polarizations of the initial photon.

For the couplings of the Majorana neutrinos we follow Ref [6] starting with rather general lagrangian densities for the interaction of N with W and light leptons l_i (e, μ, τ):

$$\mathcal{L}_{NWl} = - \sum_{j=1}^3 \frac{g B_L^{(j)}}{\sqrt{2}} \bar{l}_j \gamma^\mu P_L N W_\mu^- + h.c. \quad (1)$$

The heavy Majorana neutrino couples to the three flavors lepton with couplings proportional to B_L^j , where j labels the family. The constant g is the standard $SU(2)_L$ gauge coupling.

This B_L^j parameters will affect the final results via the combinations $H_1 = |B_L^{(1)}|^2$ and $H = \sum_{j=1}^3 |B_L^{(j)}|^2$ in the following way: The cross-section is proportional to H_1 . This proportionally came from the interaction of the initial electron with either of intermediary or final W boson (Fig.1). In the other hand the final lepton can be either of e^+ , μ^+ or τ^+ because this is allowed by the interaction lagrangian (eq.1). All these possible final states are a clear signal for intermediary Majorana neutrino and then we sum the cross section over the flavors of the final lepton. This sum produces a H factor in the numerator of the total cross section. In the other hand this cross-section also depends on H through the total width $\Gamma_{N \rightarrow all}$ (eq.10) in the Majorana neutrino propagator.

In this work we have considered the complete set of Feynman diagrams (Fig.1) that contribute at tree level to $e^-\gamma \rightarrow W^-W^-l_1^+$ ($\rightarrow jets + l_1^+$) with the light leptons $l_1^+ =$

$$e^+, l_2^+ = \mu^+, l_3^+ = \tau^+.$$

II. HELICITY AMPLITUDE

When the number of Feynman diagrams is increased, the calculation of the amplitude is a rather unpleasant task. Some algebraic forms can be used in it to avoid manual calculation, but sometimes the lengthy printed output from the computer is overwhelming, and one can hardly find the required results from it. The CALKUL collaboration [9] suggested the Helicity Amplitude Method (HAM) which can simplify the calculation remarkably and hence make the manual calculation realistic.

In this section we discuss the evaluation of the amplitudes at the tree level for $\gamma e^- \rightarrow W^- W^- l_j^+ (l_j^+ \equiv e^+, \mu^+, \tau^+)$ using the HAM. This method is a powerful technique for computing helicity amplitudes for multiparticle processes involving massless spin-1/2 and spin-1 particles. Generalization of this method which incorporates massive spin-1/2 and spin-1 particles, are given in Ref. [10]. This algebra is easy to program and more efficient than computing the Dirac algebra.

The Feynman diagrams, which contribute at the tree-level are depicted in Fig.1 and the corresponding amplitudes can be organized as follow

$$\begin{aligned} i\mathcal{M}_1(\lambda) &= iCP_N(k_3 + p_2)P_e(p_1 + k_1)T_1(\lambda) + (k_2 \leftrightarrow k_3), \\ i\mathcal{M}_2(\lambda) &= -iCP_N(k_2 - p_1)P_e(p_2 - k_1)T_2(\lambda) + (k_2 \leftrightarrow k_3), \\ i\mathcal{M}_3(\lambda) &= -iCP_W(k_3 - k_1)P_N(k_2 + p_2)T_3(\lambda) + (k_2 \leftrightarrow k_3), \\ i\mathcal{M}_4(\lambda) &= -iCP_W(k_3 - k_1)P_N(k_2 - p_1)T_4(\lambda) + (k_2 \leftrightarrow k_3), \end{aligned} \quad (2)$$

where λ is the polarization of the photon, $C = M_N \Lambda_M e g^2 B_L^1 B_L^j / 2$ (Λ_M is the phase factor in the Fourier decomposition of the Majorana field $N(x)$; $|\Lambda_M|^2 = 1$ [1]) and p_1, k_1, p_2, k_2 and k_3 are the 4-impulse of the particles e^- , γ , l^+ , W^- and W^- respectively. The corresponding propagators are

$$\begin{aligned} P_N(k) &= \frac{(k^2 - M_N^2) + iM_N\Gamma_N}{(k^2 - M_N^2)^2 + (M_N\Gamma_N)^2}, \\ P_W(k) &= \frac{1}{k^2 - m_W^2}, \\ P_f(k) &= \frac{1}{k^2 - m_f^2}, \end{aligned} \quad (3)$$

Following the Feynman rules [1] is straightforward to obtain the T amplitudes:

$$\begin{aligned} T_1 &= \bar{v}(p_1)\gamma_\mu(\not{p}_1 + \not{k}_1)\gamma_\nu\gamma_\alpha P_R v(p_2)\epsilon^\mu(k_1)\epsilon^\nu(k_2)\epsilon^\alpha(k_3) \\ T_2 &= \bar{v}(p_1)\gamma_\mu\gamma_\nu(\not{p}_2 - \not{k}_1)\gamma_\alpha P_R v(p_2)\epsilon^\mu(k_2)\epsilon^\nu(k_3)\epsilon^\alpha(k_1) \\ T_3 &= \bar{v}(p_1)\gamma_\mu\gamma_\nu P_R v(p_2) \left[g^{\mu\beta} - (k_1 - k_3)^\mu(k_1 - k_3)^\beta/m_W^2 \right] \end{aligned} \quad (4)$$

$$\begin{aligned}
& [g_{\rho\beta}(2k_3 - k_1)_\lambda + g_{\beta\lambda}(2k_1 - k_3)_\rho - g_{\lambda\rho}(k_1 + k_3)_\beta] \epsilon^\lambda(k_1) \epsilon^\nu(k_2) \epsilon^\rho(k_3) \\
T_4 = & \bar{v}(p_1) \gamma_\nu \gamma_\mu P_{R\nu}(p_2) \left[g^{\mu\beta} - (k_1 - k_3)^\mu (k_1 - k_3)^\beta / m_W^2 \right] \\
& [g_{\rho\beta}(2k_3 - k_1)_\lambda + g_{\beta\lambda}(2k_1 - k_3)_\rho - g_{\lambda\rho}(k_1 + k_3)_\beta] \epsilon^\lambda(k_1) \epsilon^\nu(k_2) \epsilon^\rho(k_3)
\end{aligned}$$

In order to calculate these amplitudes we follow the rules from helicity formalism and use identities of the type

$$\{\bar{u}_\lambda(p_1) \gamma^\mu u_\lambda(p_2)\} \gamma_\mu = 2u_\lambda(p_2) \bar{u}_\lambda(p_1) + 2u_{-\lambda}(p_1) \bar{u}_{-\lambda}(p_2), \quad (5)$$

which is in fact the so called Chisholm identity, and

$$\not{p} = u_\lambda(p) \bar{u}_\lambda(p) + u_{-\lambda}(p) \bar{u}_{-\lambda}(p), \quad (6)$$

defined as a sum of the two projections $u_\lambda(p) \bar{u}_\lambda(p)$ and $u_{-\lambda}(p) \bar{u}_{-\lambda}(p)$.

The spinor products are given by

$$\begin{aligned}
s(p_i, p_j) &\equiv \bar{u}_+(p_i) u_-(p_j) = -s(p_j, p_i), \\
t(p_i, p_j) &\equiv \bar{u}_-(p_i) u_+(p_j) = [s(p_j, p_i)]^*.
\end{aligned} \quad (7)$$

Using the above rules, which are proved in Ref. [10], we can reduce many amplitudes to expressions involving only spinor products.

In order to add up the polarization of the W vector bosons in the final state we define two auxiliary lightlike 4-vectors for each W such that $k_i = r_i^1 + r_i^2$, $(r_i^1)^2 = (r_i^2)^2 = 0$ and $(k_i)^2 = m_W^2$ ($i = 2, 3$). We also introduce the object $a_i^\mu = \bar{u}_-(r_i^1) \gamma^\mu u_-(r_i^2)$. As was shown in Ref [10] we will arrive at the correct result for the cross section if we make the following replacements for the outgoing W :

$$\begin{aligned}
\epsilon^\mu &\rightarrow a^\mu, \\
\sum_{pol} \epsilon^\mu \epsilon^{*\nu} &\rightarrow \frac{3}{8\pi m_W^2} \int d\Omega a^\mu a^{*\nu}
\end{aligned} \quad (8)$$

In order to obtain the cross section we have to perform additional two-dimensional integral but no accuracy will be lost since the accuracy of Monte Carlo integration does not depend on the dimensionality.

For the polarization of the initial photon we take [10] $\epsilon_\lambda^\mu(k) = N \bar{u}_\lambda(k) \gamma^\mu u_\lambda(p)$ where p^μ is any lightlike vector not collinear to k^μ . We take for p^μ one of the other momenta occurring in the problem. In this calculation we choose for p^μ the 4-moment of the incident electron (p_1^μ).

For simplicity in the expressions and in the numerical calculation we assign a number for each 4-moment as it is shown in Fig.1. In this conditions we represent the products $s(p_i, p_j)$ and $t(p_i, p_j)$ with the symbols s_{ij} and t_{ij} respectively. For the auxiliary moments $r_2^1, r_2^2, r_3^1, r_3^2$ we assign the numbers 4, 5, 6, 7 respectively. Using of the above rules and definitions we can write the T amplitudes as follow:

$$\begin{aligned}
T_1(+ &= 0, \\
T_1(- &= 8t_{12}s_{12}t_{24}s_{57}t_{63}, \\
T_2(+ &= 8t_{31}s_{23}t_{36}s_{75}t_{41}, \\
T_2(- &= 8t_{32}(s_{13}t_{36} - s_{12}t_{26})s_{75}t_{41}, \\
T_3(+ &= 2t_{34}(4s_{57}t_{61}(s_{26}t_{61} + s_{27}t_{71}) - 2s_{27}t_{61}(s_{56}t_{61} + s_{57}t_{71} + s_{52}t_{21}) + \\
&\quad 2t_{61}s_{27}(s_{56}t_{61} + s_{57}t_{71} - s_{52}t_{21})), \\
T_3(- &= 2t_{34}(4s_{57}t_{61}(t_{26}s_{61} + t_{27}s_{71}) - 2t_{26}s_{71}(s_{56}t_{61} + s_{57}t_{71} + s_{52}t_{21}) + 4s_{51}t_{21}t_{62}s_{27} + \\
&\quad 2t_{62}s_{17}(s_{56}t_{61} + s_{57}t_{71} - s_{52}t_{21})), \\
T_4(+ &= 2t_{41}(4t_{36}s_{75}(s_{26}t_{61} + s_{27}t_{71}) - 2s_{27}t_{61}(t_{36}s_{65} + t_{37}s_{75} + t_{32}s_{25}) + 4t_{31}s_{25}t_{62}s_{27} + \\
&\quad 2t_{61}s_{27}(t_{36}s_{65} + t_{37}s_{75} - t_{32}s_{25})), \\
T_4(- &= 2t_{41}(4t_{36}s_{75}(t_{26}s_{61} + t_{27}s_{71}) - 2t_{26}s_{71}(t_{36}s_{65} + t_{37}s_{75} + t_{32}s_{25}) + 4t_{32}s_{15}t_{62}s_{27} + \\
&\quad 2t_{62}s_{17}(t_{36}s_{65} + t_{37}s_{75} - t_{32}s_{25})),
\end{aligned} \tag{9}$$

After the evaluation of the amplitudes of the corresponding diagrams, we obtain the cross-sections of the analyzed processes for each point of the phase space. For the numerical calculation we use a Monte Carlo computer program, which makes use of the subroutine RAMBO (Random Momenta Beautifully Organized) [11].

We use the Breit-Wigner propagator for the Majorana neutrino N for different values of the mass M_N . The total width $\Gamma_{N \rightarrow \text{all}}$ of N was determined at tree level considering the dominant decay modes $N \rightarrow W^\pm l_j^\mp$:

$$\Gamma_{N \rightarrow \text{all}} = \frac{g^2 H}{(32\pi M_N^3 M_W^2)} (M_N^2 - M_W^2)(M_N^4 + M_N^2 M_W^2 - 2M_W^4) \tag{10}$$

In the next section we present our results showing the cross section for different masses and different center of mass energies. Moreover we present angular distributions of the final lepton as a function of the angle with the beam for different initial photon polarizations.

III. RESULTS

Using the helicity formalism we have very compact expressions for the amplitudes (equations 2,3 and 9). In $|\bar{M}|^2$ we average over the initial polarization of the electron and sum over the final polarization of the W and l_j^+ and over the flavor of the final lepton. Moreover an $\frac{1}{2}$ factor is included to avoid double counting of the two W when integrating over the

phase space. For the unpolarized cross-section we also have to average over the initial photon polarization. We take as inputs the values of \sqrt{s} , M_N and H_1 . The cross section is formally $\propto H_1$. The H dependence is most complicate due to the Majorana neutrino propagator. In the $M_W < M_N < \sqrt{s} - M_W$ kinematic region (Reg.I), where the intermediate Majorana neutrino may be on-shell, the total cross-section is almost independent of the H value. In the other hand in the $M_N > \sqrt{s} - M_W$ region (Reg.II), where the Majorana neutrino is off-shell, the total cross-section is approximately proportional to H . The behaviour in Reg.I is easy to realize if we make the so-called peaking approximation, in which the Breit-Wigner shape of the Majorana neutrino propagator is replaced by a delta function. In this region the H dependence in the numerator is canceled by the H factor in the total width. Considering only the relevant factors in the cross section, we have

$$\sigma = \sum_j \sigma_j \sim \cdots H_1 H \frac{1}{(q^2 - M_N^2)^2 + M_N^2 \Gamma_N^2} \cdots \quad (11)$$

where j labels the final lepton flavors. Making now the peaking approximation

$$\cdots \frac{1}{(q^2 - M_N^2)^2 + M_N^2 \Gamma_N^2} \cdots \rightarrow \frac{\pi}{M_N \Gamma_N} \delta(q^2 - M_N^2) \quad (12)$$

and since that $\Gamma \sim H$ (eq.10) then we can see that $\sigma = \sum_j \sigma_j$ is almost independent of H in Reg.I.

The Fig.2 show the M_N dependence of the unpolarized cross-section σ/H_1 at fixed \sqrt{s} for $H = 0.1$. We include the 2-body process ($\gamma e^- \rightarrow W^- N$) to check the correctness of our final 3-body calculation. In Fig.3 we show the \sqrt{s} dependence of σ/H_1 for different values of M_N keeping again $H = 0.1$.

With the helicity formalism that we have used in this calculation is easy to study distributions of the final lepton for different polarizations of the initial photon. As an illustration we present in Fig.4 the angular distribution of the final lepton for left and right photons and for different values of M_N . We have ignored the experimental difficulties of detecting the discussed process unambiguously but this kind of distributions could be useful to reject possible background and for to test no-standard coupling of this neutrinos [13].

In different classes of models [12] H_1 and H are severely restricted by available experimental data (LEP and low-energy data). This bounds are $H_1 < 0.016$ and $H < 0.122$. In this work we have used the value $H = 0.1$ which agrees with the bound over H .

To illustrate the possible impact of this process in the discovery of Majorana neutrinos we show in Fig 5 and Fig 6 the curves with constant events number in the plane (H_1, M_N) for $\sqrt{s} = 300$ GeV and $\sqrt{s} = 500$ GeV respectively. In both figures we take $H = 0.1$ and we include an upper bound for H_1 ($H_1 < 0.01$). We have considered a most restrictive value for H_1 and H that the inferred of the experimental bounds such that the considered upper bound is sufficiently restricted to make a conservative analysis of the ability of this collider to discover the nature of the heavy neutrinos. We have used the estimated luminosity [14]

for the γe^- collider of $\mathcal{L} = 100 fb^{-1}$. If we take as reasonable the threshold of 100 events then we could see signatures for Majorana neutrinos for masses lower than 250 GeV and 400 GeV for $\sqrt{s} = 300$ GeV and $\sqrt{s} = 500$ GeV respectively.

Summarizing, we calculate the cross-section for the process $\gamma e^- \rightarrow W^- W^- l_j^+$ where l_j^+ are light anti-leptons (e^+, μ^+, τ^+). We have included all the contributions considering that the intermediate Majorana neutrinos can be either on-shell or off-shell. We study the total unpolarized cross-section and the angular distribution of the final lepton for polarized initial photon. Finally we investigate the events number as a function of H_1 and M_N for $H = 0.1$ and for $\sqrt{s} = 300$ and 500 GeV. We find an important range of M_N for which would be possible to see signatures for Majorana neutrinos.

Acknowledgements

We thank CONICET (Argentina), Universidad Nacional de Mar del Plata (Argentina) and CONACyT (Mexico) for their financial supports.

REFERENCES

- [1] B. Kayser, F.Gibrat-debu, and F.Perrier, *The Physics of Massive Neutrinos* (World Scientific, Singapore, 1989)
- [2] Ernest Ma and James Pantaleone, Phys. Rev. **D40**, 2172 (1989)
- [3] A.Datta, M. Guchait and A. Pilaftsis, Phys. Rev. **D50**, 3195 (1994)
- [4] J. Gluza and M. Zralek, Phys. Rev. **D51**, 4707 (1995)
- [5] Axel Hoefer and L. M. Sehgal, Phys. Rev **D54**, 1944 (1996)
- [6] G. Cvetic, C. S. Kim and C. W. Kim, Phys. Rev. Lett. **82**, 1999.
- [7] F. M. L. Almeida Jr, Y. A. Coutinho, J.A. Martins Simoes and M. A. B. do Vale, [hep-ph/0002024](https://arxiv.org/abs/hep-ph/0002024)
- [8] T. Ohgaki, T. Takahashi and I. Watanabe, Phys. Rev. **D56** 1723 (1997).
- [9] P. De Causmaecker, R. Gastmans, W. Troost and T. T. Wu, Phys. Lett. **B105**, (1981) 215; P. De Causmaecker, R. Gastmans, W. Troost and T. T. Wu, Nucl. Phys. **B206**, (1982) 53; F. A. Berends, R. Kleiss, P. De Causmaecker, R. Gastmans, W. Troost and T. T. Wu, Nucl. Phys. **B206**, (1982) 61; D. Dankaert, P. De Causmaecker, R. Gastmans, W. Troost and T. T. Wu, Phys. Lett. **B114**, (1982) 203; F. A. Berends, P. De Causmaecker, R. Gastmans, R. Kleiss, W. Troost and T. T. Wu, Nucl. Phys. **B239**, (1984) 382; F. A. Berends, P. De Causmaecker, R. Gastmans, R. Kleiss, W. Troost and T. T. Wu, Nucl. Phys. **B239**, (1984) 395; F. A. Berends, P. De Causmaecker, R. Gastmans, R. Kleiss, W. Troost and T. T. Wu, Nucl. Phys. **B264**, (1986) 234; F. A. Berends, P. De Causmaecker, R. Gastmans, R. Kleiss, W. Troost and T. T. Wu, Nucl. Phys. **B264**, (1986) 265.
- [10] R.Kleiss and W.J.Stirling, Nucl. Phys. B262 (1985) 235-262.
- [11] R.Kleiss and W.J.Stirling, Comput.Phys.Commun.40; 359, 1986
- [12] P. Langacker and D. London, Phys. Rev. D38 886(1988). G. Bhattacharyya and A. Datta, Mod. Phys. Lett. A6 2921 (1991). E. Nardi, E. Roulet and D. Tommasini, Nucl. Phys. B386, 239 (1992).
- [13] O.Panella, C.Carimalo, Y.N.Srivastava, A.Widom, Phys. Rev. D56 5766-5775, 1977. Eiichi Takasugi, Prog. Theor. Phys. 98 977-985, 1977. O.Panella, C.Carimalo, Y.N.Srivastava, Phys. Rev. D62 015013, 2000.
- [14] Ilya F. Ginzburg [hep-ph/9907549](https://arxiv.org/abs/hep-ph/9907549)

Figure Captions

Figure 1: Feynman graph contributing to the amplitude of the $\gamma e^- \rightarrow W^- W^- l^+$ process.

Figure 2: Unpolarized cross-section as a function of the Majorana neutrino masses for different center of mass energies (200, 300 and 500 GeV). The dot-solid line represent the 2-body process for the same center of mass energies.

Figure 3: Unpolarized cross section as a function of the center of mass energies for different Majorana neutrino masses (150 and 300 GeV).

Figure 4: Angular distribution of the final lepton with the beam axis for polarized initial photon (R: right-handed, L: left-handed), for $\sqrt{s} = 300$ GeV and for two Majorana neutrino masses (150 and 300 GeV).

Figure 5: Curves with constant events number (10, 10^2 , 10^3 , 10^4 , 10^5) in the (H_1, M_N) plane for $\sqrt{s} = 300$ GeV. The dashes line represent an upper bound for H_1 .

Figure 6: The same of Fig.5 but for $\sqrt{s} = 500$ GeV.

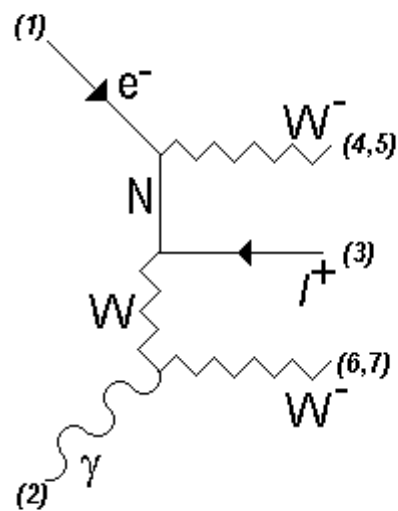
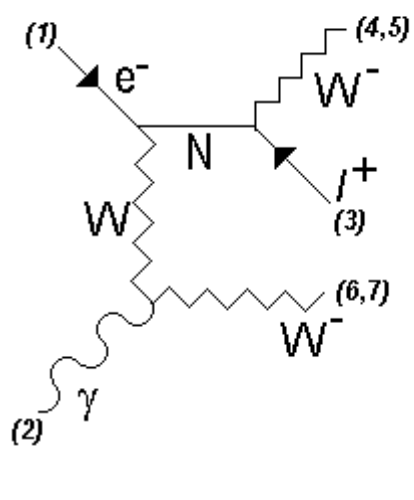
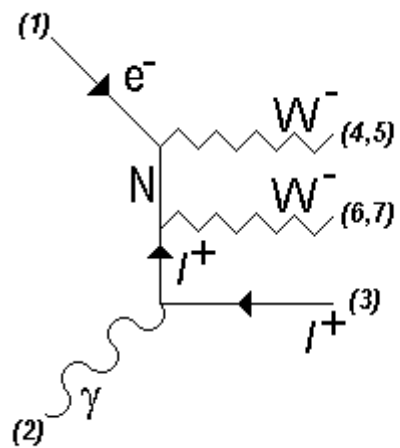
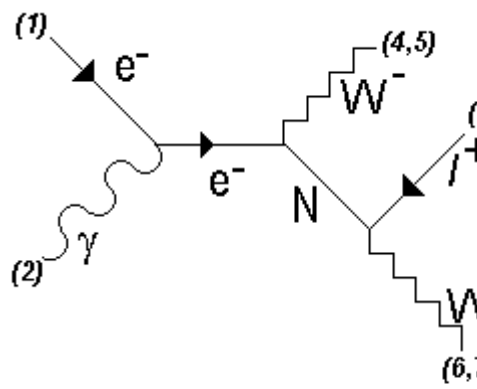


Fig. 1

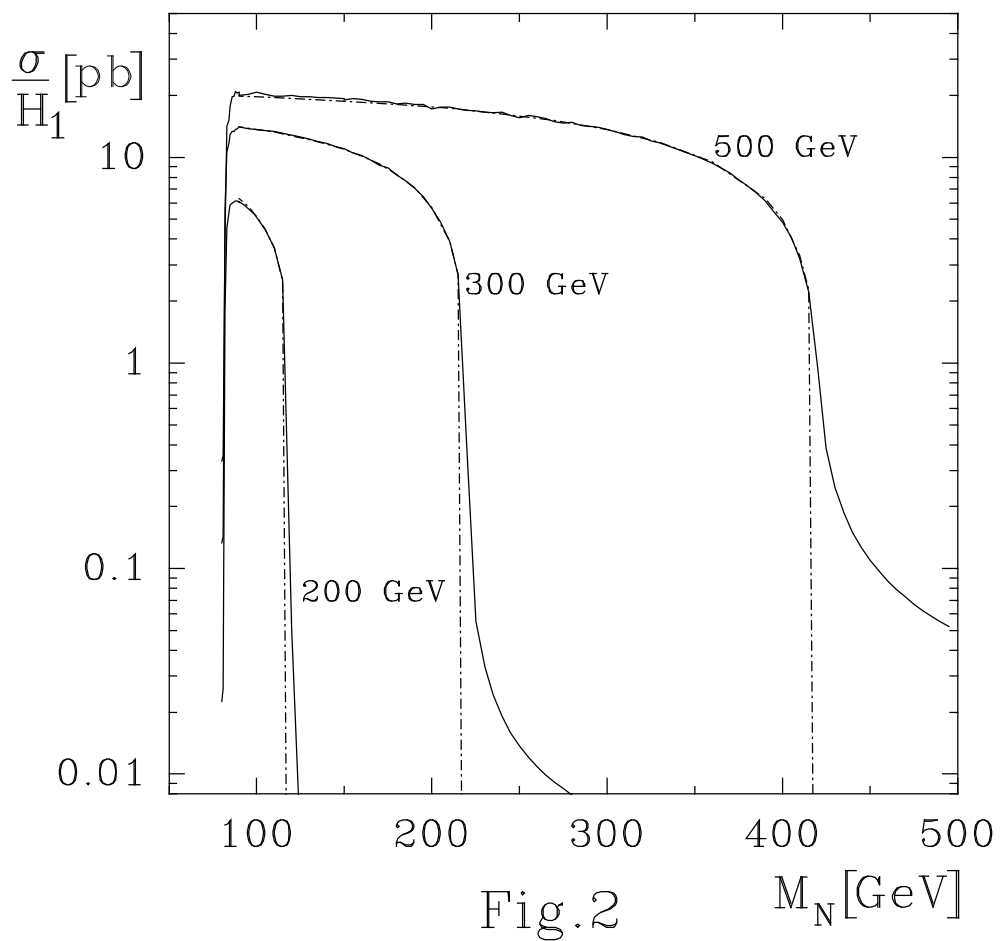


Fig.2

M_N [GeV]

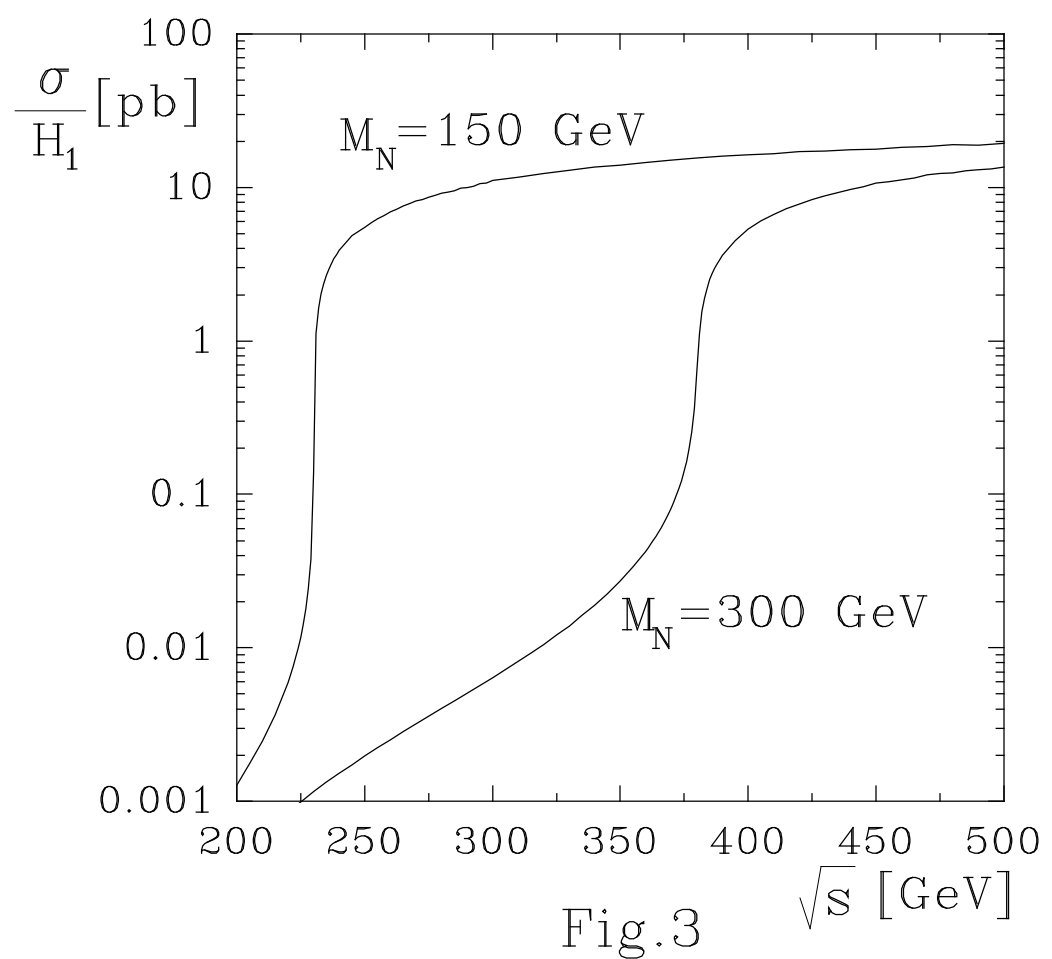
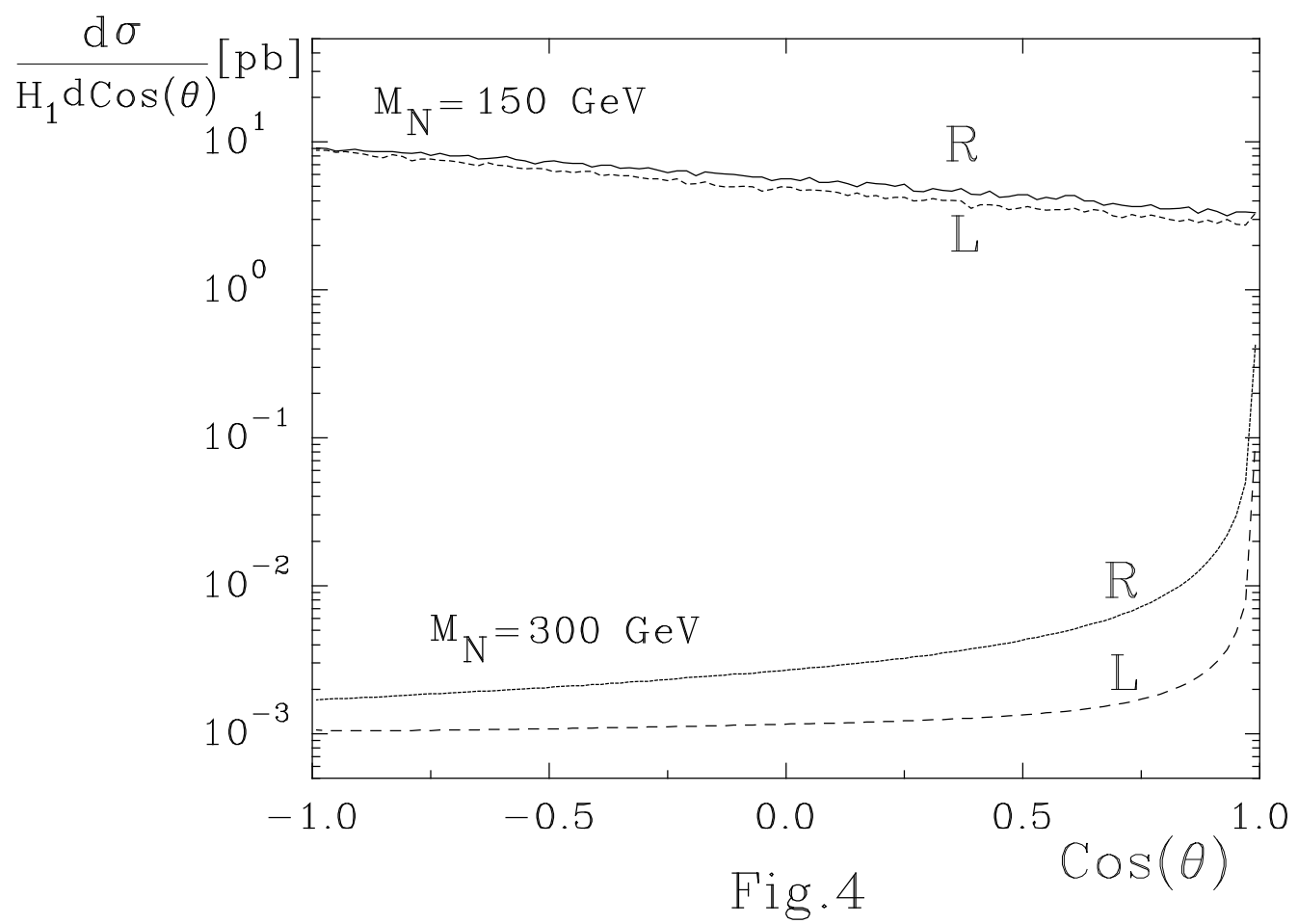


Fig.3



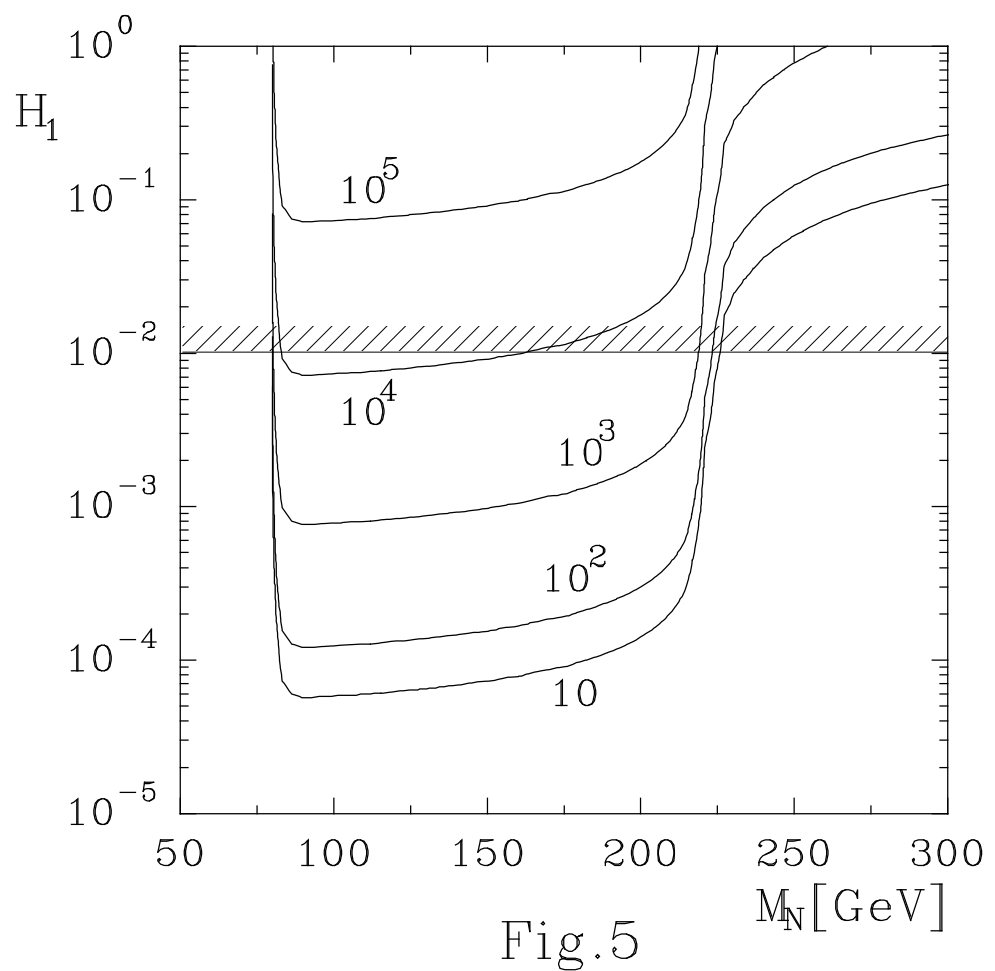


Fig. 5

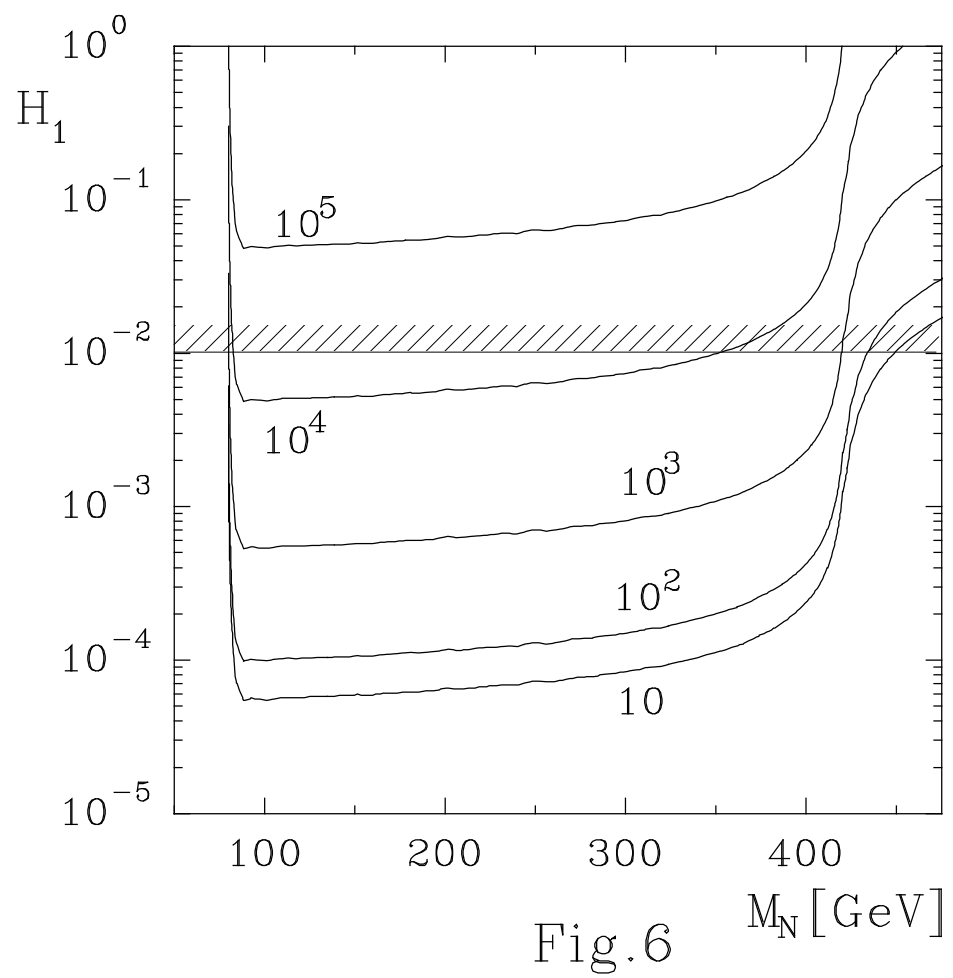


Fig. 6